International Immunopharmacology 69 (2019) 289–298

Contents lists available at ScienceDirect

International Immunopharmacology

journal homepage: www.elsevier.com/locate/intimp

BML-111 accelerates the resolution of inflammation by modulating the Nrf2/HO-1 and NF-κB pathways in rats with ventilator-induced lung injury

Jiqian Xu[a,b,d,e,1], Hong-bin Li[a,c,d,1], Lin Chen[b,d], Ya-Xin Wang[a,d], Shengzhong Lu[e], Sheng-nan Li[b,d], Shu-nan Cui[a,d], Hai-Rong Xiao[a,b,d], Lu Qin[a,b,d], Houxiang Hu[e], Shanglong Yao[b,d,*], You Shang[a,d,**]

[a] Department of Critical Care Medicine, Union Hospital, Tongji Medical College, Huazhong University of Science and Technology, Wuhan 430022, China
[b] Department of Anesthesiology, Union Hospital, Tongji Medical College, Huazhong University of Science and Technology, Wuhan 430022, China
[c] Department of Critical Care Medicine, The First Affiliated Hospital of Zhengzhou University, Zhengzhou 450052, Henan, China
[d] Institute of Anesthesiology and Critical Care Medicine, Union Hospital, Tongji Medical College, Huazhong University of Science and Technology, Wuhan 430022, China
[e] Department of Anesthesiology, North Sichuan Medical College Affiliated Hospital, Nanchong 637000, China

ARTICLE INFO

Keywords:
Ventilator-induced lung injury
Inflammation
BML-111
Neutrophil apoptosis
Pro-resolution

ABSTRACT

The timely resolution of pulmonary inflammation coordinated by endogenous pro-resolving mediators helps limit lung tissue injury, but few endogenous pro-resolving mediators that are normally operative during acute inflammation. The protective effects of BML-111 (5(*S*)-6(*R*)-7-trihydroxyheptanoic acid methyl ester), a potent commercially available anti-inflammatory and pro-resolving mediator, on ventilation-induced lung injury (VILI) have been extensively studied, but its characteristics as a pro-resolving mediator have not. Here, anesthetized Sprague-Dawley rats were ventilated with a high tidal volume (20 mL/kg, HV_T) for 1 h and randomly allocated to recover for 6, 12, 24, 48, 72, 96 or 168 h; BML-111 was administered at the peak of inflammation to evaluate its pro-resolving effect on VILI. The one-hour HV_T induced a maximal pulmonary inflammatory response at 12 h that was largely resolved by 72 h. BML-111 largely resolved the maximal inflammatory response at 48 h; the resolution interval (R*i*) was shortened by 26 h. Similarly, HV_T elicited a time course of changes in histopathology and pulmonary edema, and BML-111 alleviates these changes. Mechanistically, neutrophil apoptosis was significantly increased in BML-111-treated rats subjected to HV_T. The apoptosis inhibitor z-VAD-fmk partially reversed the proapoptotic actions of BML-111 on neutrophil and the resolving effects of BML-111 on VILI but had no effect alone. Importantly, the HV_T treatment activated the nuclear factor E2-related factor 2(Nrf2)/heme oxygenase-1(HO-1) and NF-κB signaling pathways in the lung tissue, and BML-111 further induced Nrf2 and HO-1 expression but inhibited the NF-κB pathway. Intriguingly, when we inhibited the Nrf2/HO-1 pathway with the HO-1 inhibitor zinc protoporphyrin IX (ZnPPIX), Nrf2 expression was further increased, but the inhibitory effects of BML-111 on the NF-κB pathway and on the subsequent inflammatory response, and the proapoptotic actions on neutrophil were reversed. The results suggest that BML-111 promotes the resolution of HV_T-induced inflammation to mitigate VILI in rats, perhaps by modulating the Nrf2/HO-1 and NF-κB pathways and subsequently increasing neutrophil apoptosis.

1. Introduction

Mechanical ventilation (MV) is a commonly used lifesaving therapy for critically ill patients with respiratory failure. However, MV can aggravate damage to already injured lungs and even initiate *de novo* pulmonary injury in healthy lungs, an event known as ventilator-induced lung injury (VILI) [1]. VILI is characterized by a series of inflammatory responses that are not confined to the lungs but extend to the systemic circulation and even induce multiple organ failure [2,3]. Therefore, before initiation of the pathophysiological insults, timely resolution of pulmonary inflammation is needed.

Inflammation resolution is an active, coordinated process that is

* Correspondence to: S.-L. Yao, Department of Anesthesiology, Union Hospital, Tongji Medical College, Huazhong University of Science and Technology, Wuhan 430022, China.
** Correspondence to: Y. Shang, Department of Critical Care Medicine, Union Hospital, Tongji Medical College, Huazhong University of Science and Technology, Wuhan 430022, China.
E-mail addresses: ysltian@163.com (S. Yao), you_shang@yahoo.com (Y. Shang).
[1] Jiqian Xu and Hongbin Li made equal contribution to this work.

https://doi.org/10.1016/j.intimp.2019.02.005
Received 23 July 2018; Received in revised form 21 January 2019; Accepted 4 February 2019
Available online 10 February 2019

regulated by various endogenous signaling pathways in the host, including nuclear factor E2-related factor 2 (Nrf2)/heme oxygenase-1 (HO-1) and NF-κB signaling pathways. An inducer of HO-1 promotes the resolution of inflammation, whereas an inhibitor exerts a proinflammatory effect [4]. Strategies enhancing Nrf2 activation may induce HO-1 superinduction and in turn inhibit NF-κB activation in endotoxin-activated macrophages [5]. Nrf2 deficiency exacerbates inflammatory responses and subsequent proinflammatory processes by activating NF-κB [6], and NF-κB blockers affect inflammatory resolution and enhance neutrophil apoptosis, which is paramount to an efficient resolution of inflammation [7]. Based on this evidence, crosstalk exists between the Nrf2/HO-1 and NF-κB signaling pathways and neutrophil apoptosis and thus plays an important role in modulating the resolution of inflammation.

Lipoxin A4 (LX_4) is an endogenous pro-resolving mediator involved in inflammation [8,9] and exerts a potent effect on various cell types by binding to a G protein-coupled receptor, lipoxin A4 receptor (ALX) (also termed FPRL1/FPR2) [10,11]. Activation of ALX inhibits neutrophil activation, decreases inflammatory responses evoked by a wide range of stimuli, increases anti-inflammatory macrophage cell populations and, interestingly, can intervene in apoptosis [8,12]. Because LX_4 is rapidly inactivated *in vivo*, stable and powerful analogs have been synthesized [10]. BML-111 (5(*S*)-6(*R*)-7-trihydroxyheptanoic acid methyl ester) is a commercially available ALX analog that inhibits neutrophil recruitment and reduces inflammatory responses in multiple inflammatory disorders, including pulmonary inflammation, arthritis and neuroinflammation [12–14]. BML-111 ameliorates acute pancreatitis-associated lung injury (APALI) by alleviating the inflammatory response and upregulating HO-1 expression [15] or increasing Nrf2/HO-1 activity in mice [16]. As shown in our previous study, BML-111 pretreatment inhibits NF-κB signaling in the lung tissue and reduces the number of neutrophils in the bronchoalveolar lavage fluid (BALF) in subjects with VILI [13]. Under inflammatory conditions, the number of neutrophils is increased by several factors, including the inhibition of neutrophil apoptosis [17]. Thus, the protective effect of BML-111 on lung injury may involve the Nrf2/HO-1 and NF-κB signaling pathways and neutrophil apoptosis, but whether these signaling pathways are the possible mechanism by which BML-111 affects the resolution of VILI remain unknown [18,19].

In the present study, we determined whether BML-111 promoted inflammation resolution in subjects with VILI by adapting an *in vivo* rat model of lung injury induced by high tidal volume (HV_T) ventilation for 1 h that clearly displays a time course of inflammatory changes after HV_T [20]. Furthermore, we analyzed the inflammatory resolution indices, the Nrf2/HO-1 and NF-κB signaling pathways and apoptotic neutrophils to determine the role of BML-111 in inflammation resolution.

2. Materials and methods

2.1. Animals

Specific pathogen-free adult male Sprague-Dawley rats aged 6 to 8 weeks and weighing 200 to 250 g were used (Shi lai ke jing da Company, Hunan, China). Animals were housed in a specific pathogen-free room with a controlled temperature (22–24 °C) and humidity (60–65%) on a 12-h light/dark cycle and fed a standard diet and water *ad libitum*. All experiments were conducted according to the guidelines of animal studies in China, and the study protocol was approved by the Laboratory Study Review Board of Tongji Medical College, Huazhong University of Science and Technology.

2.2. Animal model of VILI

Anesthesia was induced by an intraperitoneal injection of 120 mg/kg ketamine and 8 mg/kg xylazine. After confirmation of the depth of anesthesia with a paw clamp, animals were placed on a homeothermic blanket and were intratracheally intubated with 14-gauge intravenous catheters using previously described methods [13]. The animals were ventilated with ambient air using the Model 683 Ventilator (Harvard, Holliston, MA, USA). Anesthesia was maintained by supplementation with approximately one-fourth of the initial dose of the anesthetic agents. The animals were then allocated to ventilation at 20 mL/kg with 80 breaths/min (HV_T) for 1 h; a positive end-expiratory pressure of 0 was set for all animals subjected to ventilation to induce VILI.

2.3. Experimental protocol

BML-111 (Enzo Life Sciences, USA), z-VAD-fmk (InvivoGen, USA) and zinc protoporphyrin IX (ZnPPIX, Sigma, USA) were dissolved in dimethyl sulfoxide (DMSO, Sigma, USA) and then diluted in normal saline; the placebo control solution was saline with the same concentration of DMSO. We randomly assigned 112 rats to the HV_T group or HV_T plus BML-111 group (BML-111 group) to investigate the effects of BML-111 on the resolution of inflammation caused by HV_T. The HV_T rats were randomly allocated to assessment at eight time points (0, 6, 12, 24, 48, 72, 96 and 168 h), eight rats from each group were sacrificed at each time point. BML-111 (1 mg/kg, based on our previous experiments [13]) and an identical volume of the placebo control solution were intraperitoneally injected into the BML-111 group at 12 h following HV_T, and these rats were randomly allocated to assessment at six time points (12, 24, 48, 72, 96 and 168 h), eight rats from each group were sacrificed at each time point.

We randomly assigned rats to the sham group (rats underwent intratracheal intubation but breathed spontaneously), HV_T group, HV_T plus BML-111 group (BML-111), HV_T plus pan-caspase inhibitor z-VAD-fmk group (z-VAD), and HV_T plus BML-111 and z-VAD-fmk group (BML-111 + z-VAD-fmk) to study the role of neutrophil apoptosis in BML-111-mediated resolution of HV_T-induced VILI, eight rats for each group. Rats were intraperitoneally administered BML-111 (1 mg/kg) or an identical volume of the placebo control solution 12 h after the end of HV_T. The animals in the BML-111 plus z-VAD-fmk group were intraperitoneally injected with z-VAD-fmk (10 μg/kg) at the end of HV_T, followed by injections with two additional doses of z-VAD-fmk 4 and 8 h later [21]. The rats in the other groups received injections of the placebo control solution at the same volume. Twenty-four hours after the end of HV_T, approximately 1 mL of arterial blood was withdrawn from the left carotid artery into a heparinized syringe. The PaO_2 levels were determined immediately with a blood gas analyzer, and the lungs were harvested or lavaged for further analysis.

Rats were randomly assigned to the sham group, HV_T group, HV_T plus BML-111 group (BML-111), HV_T plus HO-1 specific inhibitor ZnPPIX group (ZnPPIX) and HV_T plus BML-111 and ZnPPIX group (BML-111 + ZnPPIX) to investigate the role of the Nrf2/HO-1 signaling pathway in the BML-111-mediated resolution of HV_T-induced VILI, six rats for each group. Rats were intraperitoneally administered ZnPPIX (20 mg/kg, Sigma, USA) or an identical volume of the placebo control solution 1 h before HV_T, as described in a previous study [22]. Rats in the other groups received injections of the identical volume of the placebo control solution. Twenty-four hours after the end of HV_T, the lungs were harvested or lavaged for further analysis.

2.4. Lung histological assays

At the indicated time points, rats were sacrificed by injecting three times the normal dose of ketamine, the thorax was carefully dissected by midline sternotomy, and the upper right lung was isolated, fixed with 4% paraformaldehyde and embedded in paraffin wax. Sections that were approximately 4-μm thick were stained with hematoxylin and eosin. Lung injury scores were determined by an investigator who was blinded to the treatment groups using recently published criteria [23].

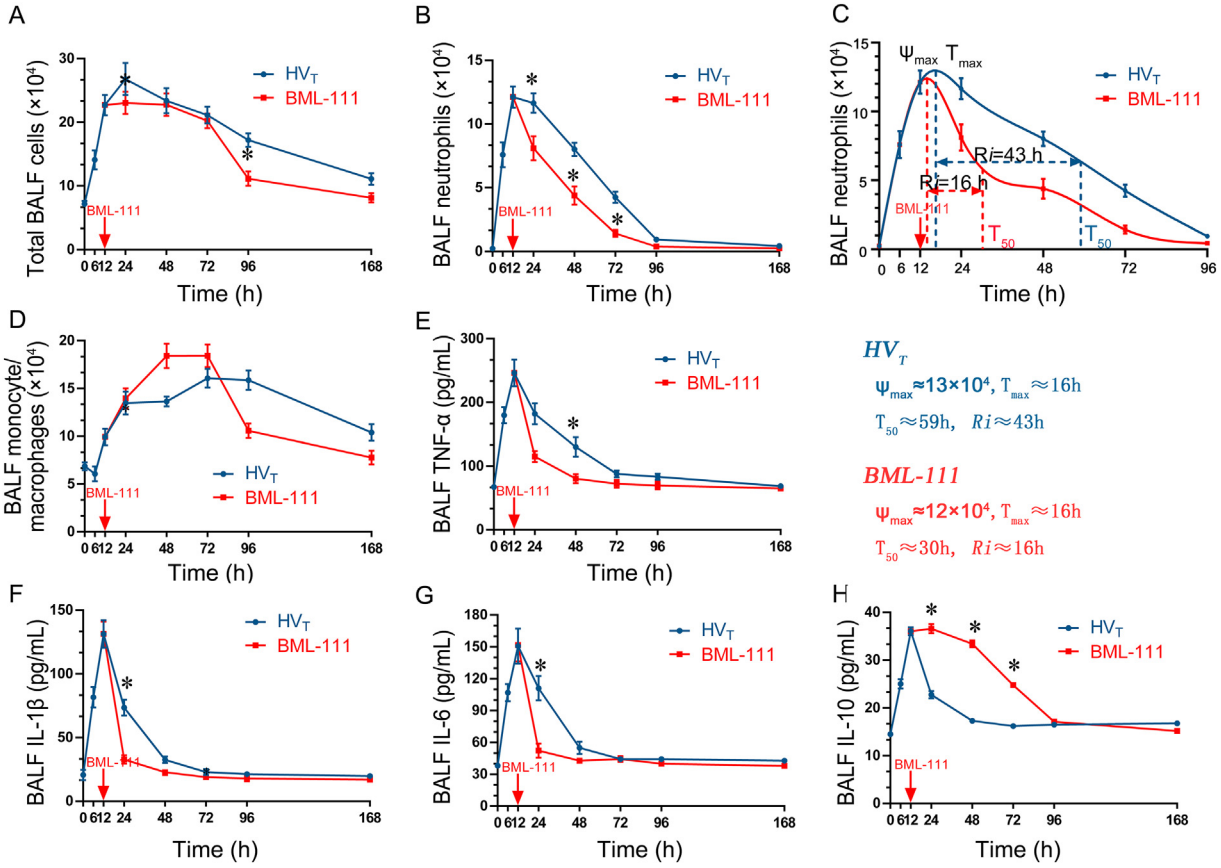

Fig. 1. Time course of the deterioration of indices of lung injury and effects of BML-111. Twelve hours after the end of HV_T, rats were administered intraperitoneal injections of NS or BML-111 (1 mg/kg) and sacrificed at the indicated time points. Lung tissues from rats subjected to HV_T (0 and 6 h following HV_T) and rats subjected to HV_T treated with BML-111 or saline (12, 24, 48, 72, 96 and 168 h following HV_T) were evaluated for histopathological changes and lavaged to analyze the BALF. (A) Representative micrographs of hematoxylin-eosin staining of lung sections (magnification, 200×). (B) Lung injury scores. (C) Lung wet/dry weight ratio. (D) BALF protein concentrations. Data are presented as the means ± SEM (n = 8 animals per group). $^*P < 0.05$ compared with the HV_T group.

2.5. Measurements of the lung water content and total protein concentration in the BALF

The lung water content related to lung injury was measured using the lung wet-to-dry weight ratio as previously described [13]. The middle lobe of the right lung was weighed immediately after removal (wet weight) before bronchoalveolar lavage (BAL) collection, and the lung was dried in an oven for 72 h at 60 °C before reweighing (dry weight).

BALF was collected as previously described [13]. Briefly, the left lungs were lavaged three times with 2.5 mL of ice-cold lavage buffer (phosphate-buffered saline containing 0.6 mM EDTA). The lavage was centrifuged at 4 °C for 10 min at 1500 rpm, and cells in the BALF were resuspended in 1 mL of phosphate-buffered saline for the analyses described below. Total protein in cell-free BALF was assayed as an index of lung injury and capillary leakage. Protein concentrations were measured with the BCA Protein Assay Reagent Kit (Pierce Biotechnology, Rockford, IL, USA).

2.6. Differential leukocyte counts and cytokine analysis

The total cell number per milliliter of BALF was determined with a hematocytometer. Next, approximately 5×10^4 cells from each BALF sample were placed on a microscope slide and centrifuged at 800 rpm for 10 min at room temperature using Cytospin (Thermo Shandon, Pittsburgh, PA, USA). Then, the slides were air-dried and stained with Giemsa-Wright, and at least 300 cells were counted under a light microscope for the differential cell count analysis. Moreover, to quantify the local kinetics of leukocyte infiltration, we determined the resolution indices (R*i*) using previously described methods [8,24,25]. The concentrations of interleukin-1β (IL-1β), interleukin-6 (IL-6), tumor necrosis factor-α, and interleukin-10 (IL-10) in the BALF were measured using enzyme-linked immunosorbent assays (eBioscience Inc., San Diego, CA, USA) according to the manufacturer's instructions.

2.7. Assessment of neutrophil apoptosis in the BALF

Cells were labeled with an APC-conjugated anti-annexin-V antibody and FITC-conjugated Gr-1 antibody (Abcam, Cambridge, MA, USA) for 30 min to evaluate neutrophil apoptosis in the BALF. The annexin-V^+ Gr-1^+ neutrophil population was enumerated using flow cytometry.

2.8. Measurement of HO-1 activity

The HO-1 activity in lung tissues was measured as reported in a previous study [22,26]. Briefly, lung tissues were homogenized on ice with homogenization buffer (1 M Tris-HCl, 250 mM sucrose) and centrifuged at 4 °C for 30 min (12,000 × *g*). The supernatant (200 μL) was collected and incubated with 100 μL of liver cytosol (a source of biliverdin reductase), 0.8 mM NADPH (Sigma, USA), and 20 mM hemin. The reaction was conducted at 37 °C in the dark for 40 min and terminated by placing the samples on ice for 10 min. The absorbance was measured at 464 and 530 nm. The amount of bilirubin formed was calculated from the difference in absorbance at 464 and 530 nm. HO-1 activity was expressed as pmol bilirubin mg $\text{protein}^{-1}\,\text{h}^{-1}$.

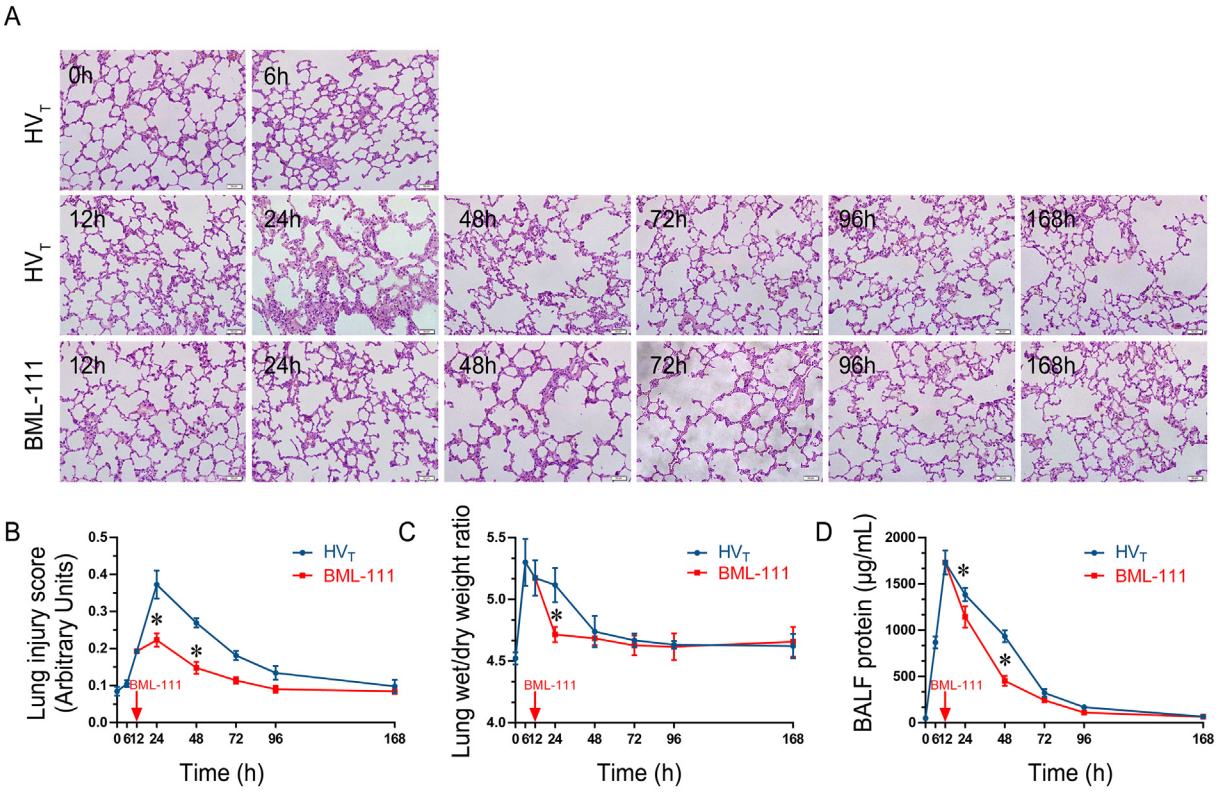

Fig. 2. Time course of inflammation resolution following HV_T and effects of BML-111. Twelve hours after the end of HV_T, rats were administered intraperitoneal injections of NS or BML-111 (1 mg/kg) and sacrificed at the indicated time points. The BALF and the cells in BALF from rats subjected to HV_T (0 and 6 h following HV_T) and rats subjected to HV_T and treated with BML-111 or saline (12, 24, 48, 72, 96 and 168 h following HV_T) were collected at the indicated time points. The inflammatory cells were enumerated under a light microscope, and cytokine levels were measured using ELISA kits. (A) Total leukocytes. (B) Neutrophil counts. (C) Resolution indices of neutrophil infiltration: Ψ_{max} (neutrophil infiltration maximum count), T_{max} (time interval for neutrophils to reach the maximum count), T_{50} (time interval corresponding to a 50% neutrophil reduction), and R*i* (interval between Ψ_{max} and T_{50}). (D) Monocyte/macrophage counts. (E) TNF-α, (F) IL-1β, (G) IL-6 and (H) IL-10 levels. Data are presented as means ± SEM (n = 8 animals per group). *$P < 0.05$ compared with the HV_T group.

Table 1
Changes in Resolution Indices by BML-111 treatment.

Group	T_{max} (h)	Ψ_{max} (PMN No. × 10^4 cells)	T_{50} (h)	Ψ_{50} (PMN No. × 10^4 cells)	R*i* (h)
HV_T	16.20 ± 0.80	12.99 ± 0.84	58.80 ± 1.42	6.29 ± 0.72	42.60 ± 1.50
BML-111	13.61 ± 0.75	12.37 ± 0.95	29.95 ± 1.16*	5.75 ± 0.69	16.35 ± 1.02**

Data represent the mean ± SEM (n = 6) and were analyzed with the two-tailed Student's *t*-test. Ψ_{max} = maximal polymorphonuclear leucocyte (PMN) number; T_{max} = time point when the number of PMNs reached Ψ_{max}; T_{50} = time point when PMN numbers decreased to 50% Ψ_{max}; R*i* = time interval from the maximum PMN point (Ψ_{max}) to the 50% reduction point (R_{50}).

* $P < 0.05$ compared with the HV_T group.

** $P < 0.01$ compared with the HV_T group.

2.9. Western blot analysis

The whole-cell lysates and the protein concentrations were observed as previously described [13], the nuclear and cytoplasmic proteins were extracted from the lung tissues using the NE-PER Nuclear and Cytoplasmic Extraction Reagents (Pierce Biotechnology) according to the manufacturer's instruction. Equal volumes and amounts of protein were separated by electrophoresis and subsequently transferred to PVDF membranes (Millipore. Billerica, MA) by electroblotting using previously reported methods [27]. After blocking with 5% fat-free dry milk in Tris-buffered saline (TBS) containing 0.1% Tween-20 (TBST) for 1 h at room temperature, membranes were incubated with primary antibodies overnight at 4 °C. PVDF membranes were washed with TBST and subsequently incubated with horseradish peroxidase (HRP)-conjugated secondary antibody at room temperature for 1 h, followed by ECL detection and quantification using an image analysis program. Antibodies against Nrf2 and HO-1 were purchased from Cell Signaling Technology (Danvers, MA, USA). NF-κB, IκB, β-actin, and horseradish peroxidase-conjugated anti-rabbit antibodies were purchased from Santa Cruz Biotechnology. The lamin B1 antibody was purchased from Epitomics (Burlingame, CA, USA).

2.10. Statistical analysis

Results are presented as means ± SEM. Data were analyzed using SPSS software version 17.0 (SPSS, Inc., Chicago, IL, USA). Data were analyzed with one-way analysis of variance followed by the least significant difference *post hoc* test or Tukey's *post hoc* multiple comparison test, when appropriate. The criterion for significant differences was set to $P < 0.05$ for all studies.

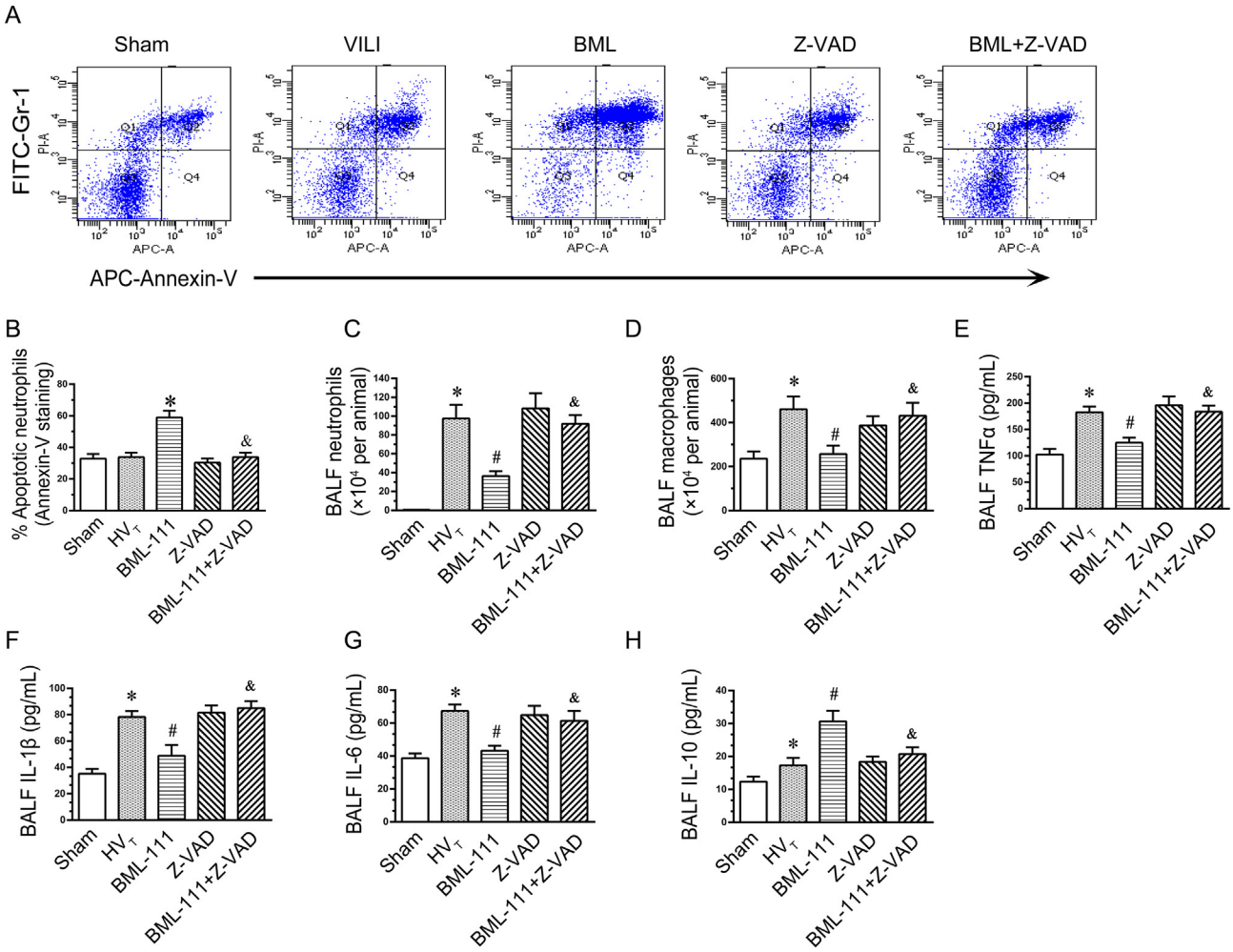

Fig. 3. Effects of inhibiting neutrophil apoptosis on the BML-111-induced resolution of inflammation caused by HV_T. Animals in the BML-111 + Z-VAD group were intraperitoneally injected with the pan-caspase inhibitor z-VAD-fmk (10 μg/kg in 0.2 mL of saline) immediately at the end of HV_T and with two additional doses of z-VAD-fmk 4 and 8 h later. The other groups were intraperitoneally injected with NS or BML-111 (1 mg/kg). BALF was collected by flushing the lungs of rats sacrificed 24 h after HV_T. (A) Flow cytometry analysis of neutrophil apoptosis. Cells in BALF were labeled with APC-annexin-V and FITC-Gr-1 antibodies. Apoptotic neutrophils (annexin-V^+ Gr-1^+) are indicated in the upper right quadrant. (B) Percentage of apoptotic neutrophils. (C) Neutrophils and (D) monocytes/macrophages were enumerated under a light microscope, and the levels of TNF-α (E), IL-1β (F), IL-6 (G) and IL-10 (H) in BALF were measured using ELISA kits. Data are presented as the means ± SEM (n = 8 animals per group). $^*P < 0.05$ compared with the sham group, $^{\#}P < 0.05$ compared with the HV_T group, and $^{\&}P < 0.05$ compared with the BML-111 group.

3. Results

3.1. Effect of BML-111 on the resolution of VILI

Sprague-Dawley rats were subjected to HV_T and underwent periods of recovery of 6, 12, 24, 48, 72, 96 or 168 h to confirm whether the protective effect of BML-111 on VILI was associated with its pro-resolving role. The progressive increase in lung injury histological indices peaked at 24 h, with resolution up to 7 days later in HV_T-treated rats. Histopathological changes in BML-111-treated rats differed from those in HV_T-treated rats and included disturbed alveoli and neutrophil infiltration, which were alleviated and recovered to normal on day 4. Representative images of lung histology at each time point following HV_T are shown in Fig. 1A. Lung injury scores that correlated with the changes are shown in Fig. 1B. Pulmonary edema was indicated by the lung wet/dry weight ratio and the amount of BALF proteins. The lung wet/dry weight ratio peaked at 6 h and gradually decreased, approaching normal levels at 24 h, and the amount of BALF proteins peaked at 12 h and gradually recovered up to 48 h later (Fig. 1C and D). These changes were alleviated by BML-111 (Fig. 1C and D) and recovered to normal levels sooner than in HV_T-treated rats. These time-course data suggest that BML-111 propagates the resolution of VILI.

3.2. BML-111 propagates the resolution of inflammation caused by HV_T

The timely resolution of lung inflammation is one of the major factors contributing to the resolution of lung injury. Our results showed that the number of leukocytes and neutrophils rapidly increased, plateaued at 12 h and then gradually decreased to normal levels up to 4 days later (Fig. 2A and B), and the levels of TNF-a, IL-1β, IL-6 and IL-10 in the BALF raised rapidly and plateaued at 12 h and then gradually decreased, thus BML-111 was administered 12 h after HV_T, and BML-111 treatment resulted in significant decreases in exudate leukocytes and neutrophil infiltration (from ~12×10^4 to ~8×10^4 at 24 h, respectively); the counts returned to baseline levels after 3 days, and the levels of proinflammatory cytokines TNF-a, IL-1β, and IL-6 in the BALF was significantly reduced than that of the HV_T model (Fig. 2E, F and G), but the level of the anti-inflammatory cytokine IL-10 (Fig. 2H) was maintained at a higher level in the BALF of the BML-111 group than in the HV_T group. To quantify the resolution speed and quantitatively analyze the role of BML-111 in inflammation resolution, we used the resolution interval (R_i), which is defined as the time period in which the

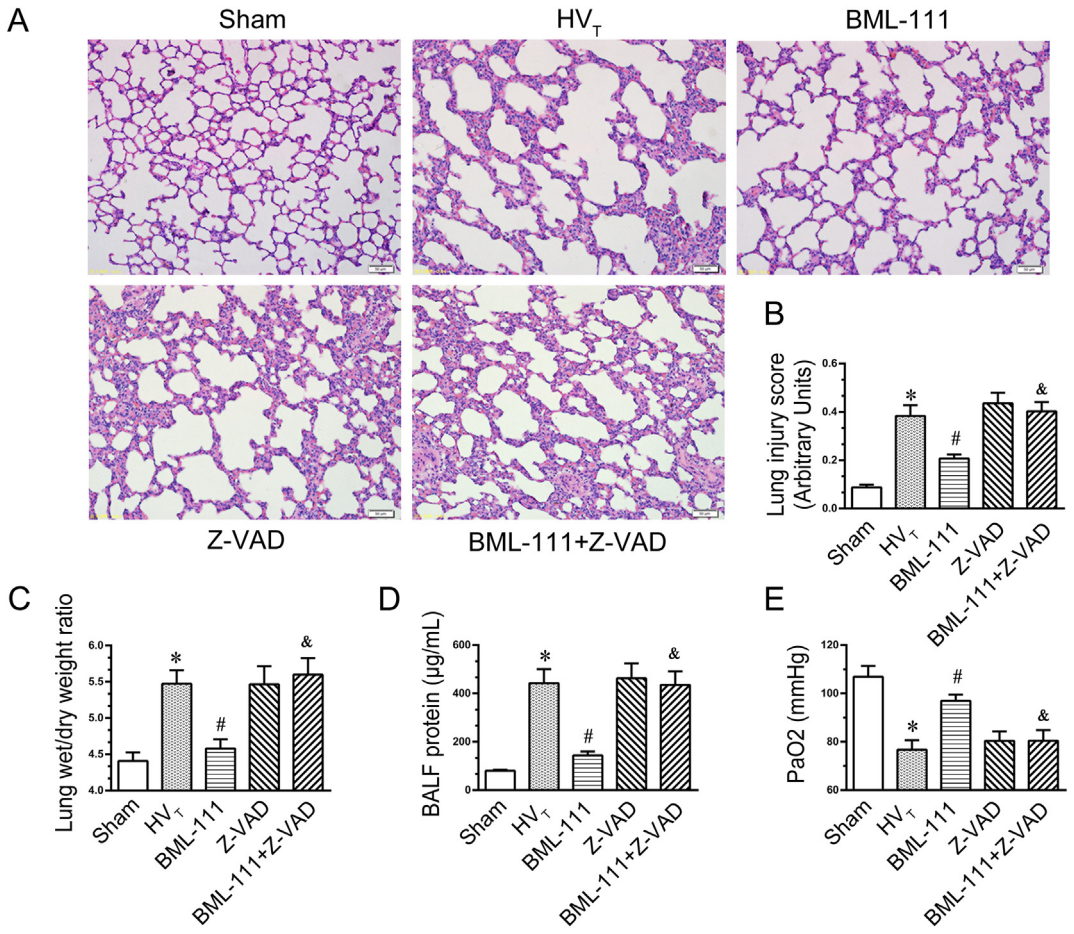

Fig. 4. Effects of the apoptosis inhibitor z-VAD-fmk on the pro-resolving effects of BML-111 on VILI in rats. Animals in the BML-111 + Z-VAD group were intraperitoneally injected with the pan-caspase inhibitor z-VAD-fmk (10 μg/kg in 0.2 mL of saline) at the end of HV_T, with two additional doses of z-VAD-fmk administered 4 and 8 h later. The other groups were intraperitoneally injected with NS or BML-111 (1 mg/kg). Lung tissues were evaluated for histopathological changes and lavaged for an analysis of the BALF 24 h after HV_T. Representative images of hematoxylin-eosin-stained lung tissue sections (magnification, 200 ×) (A), lung injury scores (B), lung wet/dry weight ratio (C), BALF protein concentrations (D) and arterial oxygen pressures (E). Data are presented as the means ± SEM (n = 8 animals per group). $^*P < 0.05$ compared with the sham group, $^{\#}P < 0.05$ compared with the HV_T group, and $^{\&}P < 0.05$ compared with the BML-111 group.

neutrophil number is reduced from the maximum number to 50%, [8,24,25]. The lungs of the HV_T model had a R_i of ~43 h, ranging from 16 h (T_{max}) to 59 h (T_{50}) (Fig. 2C and Table 1), and the BML-111 treatment significantly shortened the R*i* (from 14 to 30 h). Monocytes and macrophages play critical roles in the initiation, maintenance and resolution of inflammation. HV_T caused a steady increase in the macrophage/monocyte counts, followed by a rapid decrease, until these cells became the predominant exudate leukocytes at 72 h. The counts did not decrease to baseline levels at 168 h (Fig. 2D) in the HV_T group. BML-111 administration shifted the peak in the maximum number of macrophages/monocytes to 48 h after HV_T, with a subsequent rapid decrease, and the counts also approached normal levels (Fig. 2D). Based on these data, BML-111 accelerates inflammation resolution following VILI.

3.3. Inhibition of neutrophil apoptosis with the caspase inhibitor z-VAD-fmk attenuates the pro-resolving effects of BML-111 on inflammation and VILI

Neutrophil apoptosis plays a vital role in the resolution of inflammation and lung injury [17]. Based on the results described above, the lung injury caused by neutrophil-mediated inflammation peaked at 24 h. Therefore, we detected neutrophil apoptosis 24 h after HV_T exposure and observed a low percentage of apoptotic neutrophils in the sham and HV_T groups. The BML-111 treatment significantly increased the number of annexin-V^+ Gr-1^+ cells compared with the sham and HV_T groups (Fig. 3A and B). The activation of caspase family members is crucial for the initiation, propagation, and execution of apoptosis. We used the general caspase inhibitor z-VAD-fmk to further confirm the role of the increased neutrophil apoptosis associated with BML-111 in the resolution of VILI. The z-VAD-fmk treatment inhibited BML-111-induced neutrophil apoptosis compared with the BML-111-treated rats following HV_T, whereas z-VAD-fmk alone did not markedly contribute to neutrophil apoptosis. Moreover, the decreased numbers of neutrophils and macrophages, the decreased levels of proinflammatory cytokines, including TNF-α, IL-1β, and IL-6, and the increased levels of the anti-inflammatory cytokine IL-10 observed after BML-111 administration following HV_T were partially reversed by the z-VAD-fmk treatment (Fig. 3C–H). Additionally, z-VAD-fmk attenuated the protective effects of BML-111 on alleviating histopathological changes (Fig. 4A and B), pulmonary edema (Fig. 4C and D) and PaO_2 (Fig. 4E) in rats with HV_T-induced VILI. Similarly, z-VAD-fmk had no significant effect on VILI or the inflammatory response induced by HV_T (Fig. 4A–F). Thus, the pro-resolving effect of BML-111 on VILI may depend on neutrophil apoptosis.

3.4. The enhanced pro-resolving effects of BML-111 on VILI are partially inhibited by the HO-1 inhibitor ZnPPIX

Neutrophil apoptosis is exquisitely sensitive to stimuli from the inflammatory microenvironment, and it is regulated by various

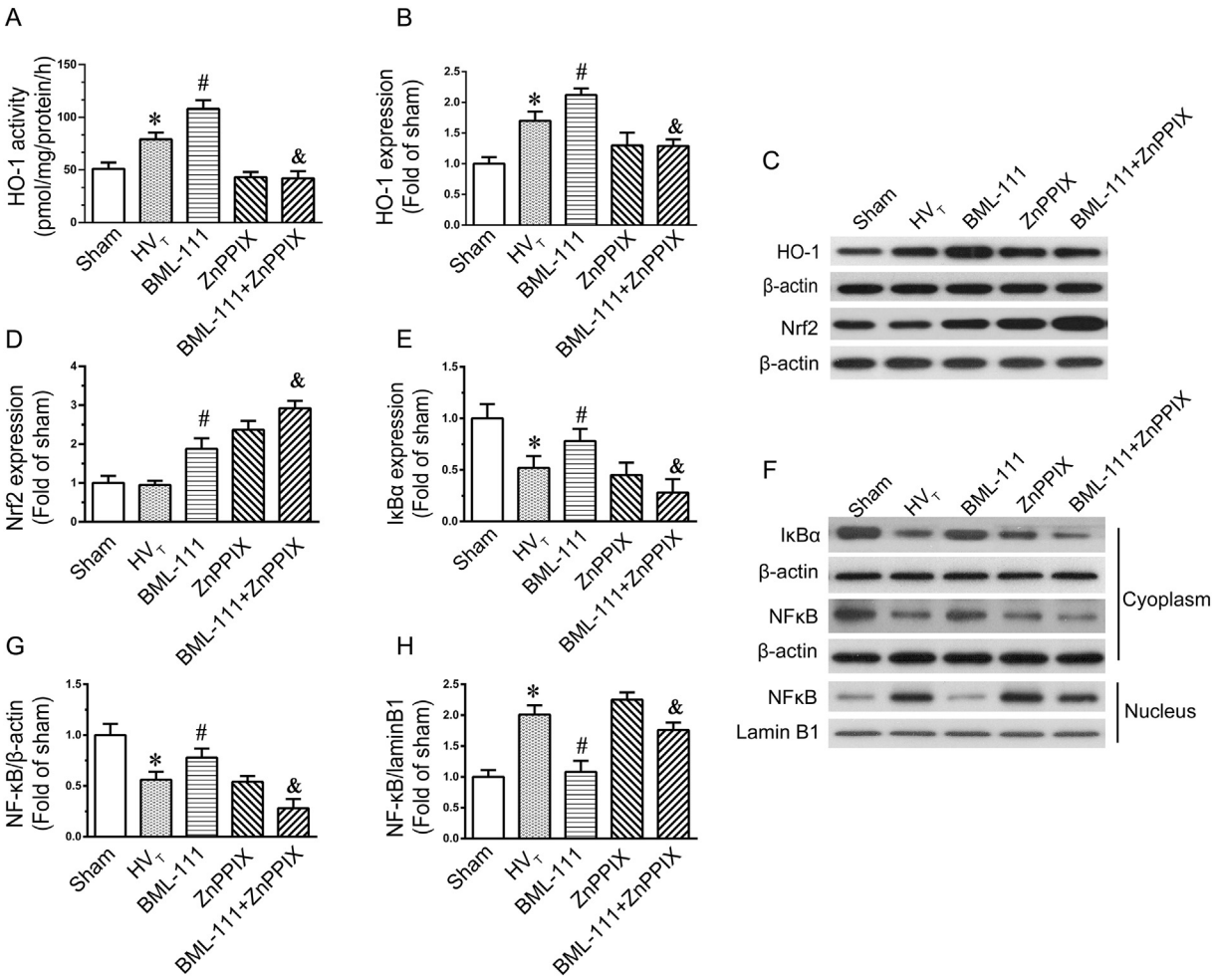

Fig. 5. Effects of the increase in Nrf2/HO-1 expression induced by BML-111 on the NF-κB signaling pathway in the VILI model. Animals in the BML-111 + ZnPPIX group were intraperitoneally injected with ZnPPIX (20 mg/kg in 0.2 mL of saline) before BML-111 administration. The other groups were intraperitoneally injected with the identical volume of the placebo control solution. Lung tissues were collected to evaluate protein expression and activity 24 h after HV_T. The activity of HO-1 (A), representative images and quantification of HO-1 expression (B and C), representative images and quantification of cytoplasmic Nrf2 levels (D and C), representative images and quantification of IκBα levels (E and F), representative images and quantification of cytoplasmic NF-κB p65 levels (G and F) representative images and quantification of nuclear NF-κB p65 levels (H and F). Data are presented as the means ± SEM (n = 6 animals per group). $^{*}P < 0.05$ compared with the sham group, $^{\#}P < 0.05$ compared with the HV_T group, and $^{\&}P < 0.05$ compared with the BML-111 group.

intracellular signaling pathways in the host, including Nrf2/HO-1 and NF-κB signaling [4,7]. We detected Nrf2 and HO-1 expression to further investigate the roles of these signaling pathways in the pro-resolving effects of BML-111. The levels of the HO-1 proteins and HO-1 activity were slightly increased in rats after mechanical ventilation than that of sham group, but the Nrf2 expression has no significant change (Fig. 5A–D). The BML-111 treatment further increased the activity of the HO-1 and the levels of the HO-1 and Nrf2 protein compared with the sham group and HV_T alone (Fig. 5A–D). Moreover, one hour's HV_T significantly decreased the expression of IκB-α expression and caused obvious translocation of NF-κB p65 from the cytoplasm into the nucleus than those of sham group, and BML-111 obviously reversed the changes (Fig. 5E–H). HO-1 expression is regulated by Nrf2, and HO-1 inhibits the NF-κB-mediated inflammatory response [4,7,16]. We thus selected ZnPPIX, a selective HO-1 inhibitor, to further verify the effect of BML-111 on resolving VILI, and we found that Nrf2 expression was still significantly increased in BML-111-treated rats subjected to HV_T following ZnPPIX administration compared with the sham and BML-11 groups (Fig. 5C and D). However, the levels and activity of the HO-1 protein were decreased in rats treated with BML-111 and ZnPPIX (Fig. 5A, B and C). Additionally, as shown in Fig. 5E–H, ZnPPIX significantly abolished the restoration of IκB expression and NF-κB nuclear translocation elicited by BML-111 after HV_T compared with the HV_T group. Furthermore, the protective effect of BML-111 on HV_T-induced changes in the levels of inflammatory cytokines and chemokines were reversed by ZnPPIX (Fig. 6A–G). Importantly, ZnPPIX reversed the effects of BML-111 on neutrophil counts, neutrophil apoptosis (Fig. 6H and I), and VILI (Fig. 6J–K). However, significant changes in the inflammatory response, neutrophil apoptosis and VILI were not observed in the ZnPPIX group compared with the HV_T group (Fig. 6A–I). Based on these results, BML-111-induced activation of the Nrf2/HO-1 pathway modulates its inhibition of the NF-κB signaling and plays an important role in the protective effects of BML-111 on VILI.

4. Discussion

The MV-triggered inflammatory response may induce tissue injury and subsequent multiple system organ dysfunction [2,25]. Timely resolution of the inflammatory response that is coordinated by endogenous pro-resolving mediators is critical for limiting excessive tissue injury [28], but few endogenous pro-resolving mediators that are normally operative during acute inflammation endogenous [29]. A synthetic analog of a pro-resolution lipid mediator, BML-111, promotes the resolution of neuroinflammation [12] and attenuates APALI by

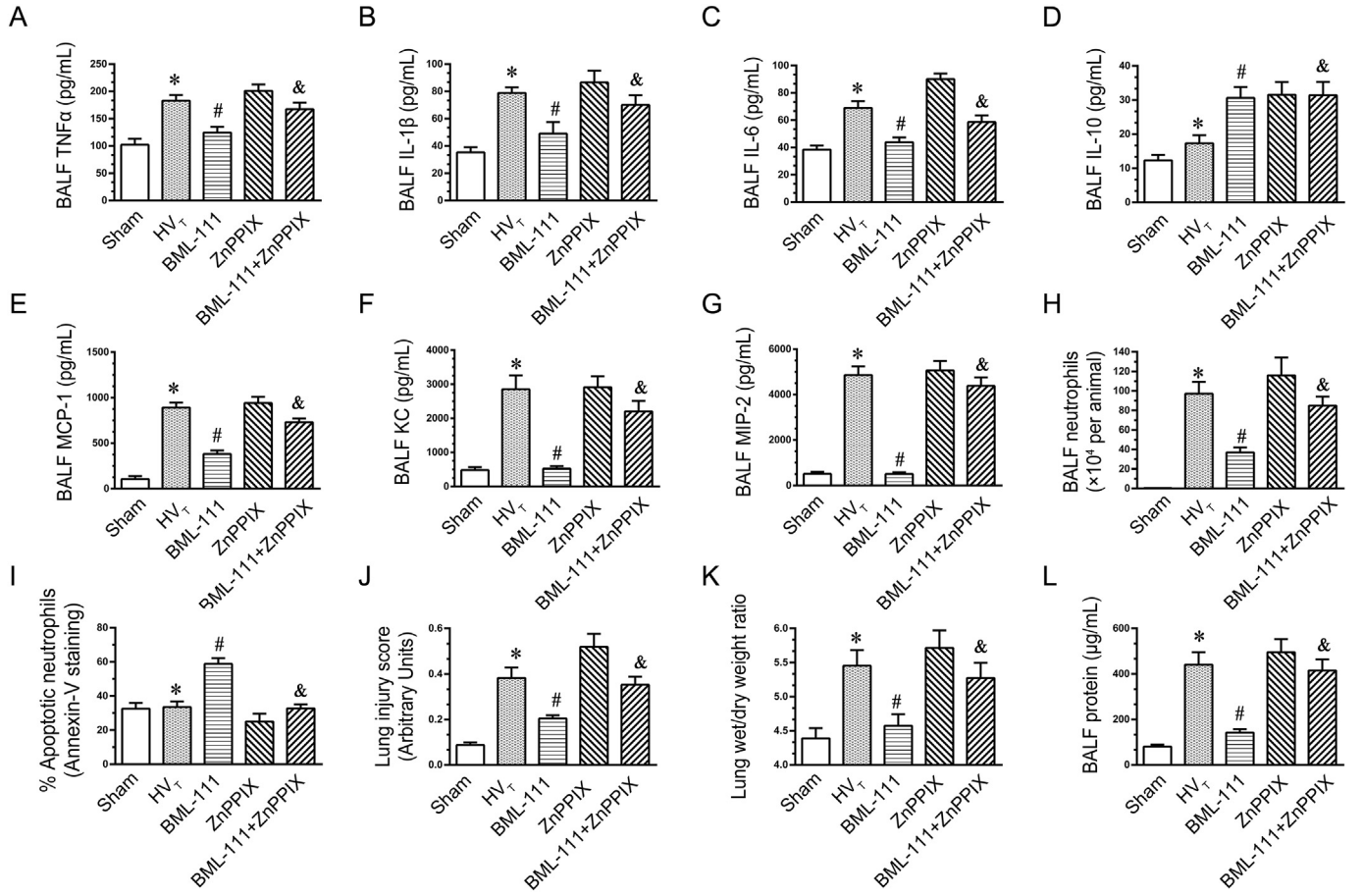

Fig. 6. The pro-resolving effects of BML-111 on VILI were partially reversed by the HO-1 inhibitor. Animals in the BML-111 + ZnPPIX group were intraperitoneally injected with ZnPPIX (20 mg/kg in 0.2 mL of saline) before BML-111 administration. The other groups were intraperitoneally injected with the identical volume of the placebo control solution. Lung tissue was lavaged for an analysis of the BALF and evaluated for histopathological changes 24 h after HV_T. The levels of TNF-α (A), IL-1β (B), IL-6 (C), IL-10 (D), MCP-1 (E), KC (F) and MIP-2 (G) in the BALF were measured using ELISA kits, and neutrophils were enumerated under a light microscope (H). Neutrophil apoptosis was evaluated using flow cytometry analysis (I). Lung injury scores (J), lung wet/dry weight ratio (K), and BALF protein levels (L) are shown. Data are presented as the means ± SEM (n = 6 animals per group). $^{*}P < 0.05$ compared with the sham group, $^{\#}P < 0.05$ compared with the HV_T group, and $^{\&}P < 0.05$ compared with the BML-111 group.

regulating the inflammatory response and HO-1 expression [15] or the Nrf2/antioxidant responsive element (ARE) signaling pathway [16]. In the present study, we selected an HV_T model with low mortality over time that is characterized by a temporal sequence of events, including organ-specific leukocyte recruitment, proinflammatory cytokine production and end-organ injury, allowing investigations into the resolution processes from this highly injured baseline. As shown in the present study, BML-111 promoted the resolution of inflammation following HV_T by regulating the Nrf2/HO-1 and NF-κB pathways in rats.

MV-induced neutrophilic alveolitis is central to the resolution of the inflammatory response [30,31]. Our results revealed the pro-resolving effects of BML-111 on the inflammatory response, including decreased the neutrophil amounts and levels of TNFα, IL-1β and IL-6. To quantitatively analyze the effect of BML-111 on inflammation resolution in the VILI model, we used the resolution indices introduced by previous studies [8,24,25]. These indices included Ψ_{max}, the maximal neutrophil number present during the inflammatory response; T_{max}, the time point when neutrophils reach Ψ_{max}; and R_i, the time interval between T_{max} and T_{50} when neutrophil numbers reach half Ψ_{max}. A quantitative analysis of the resolution of inflammation showed that a posttreatment with BML-111 shortened the R_i. Neutrophil-mediated inflammation contributes to the initiation of monocyte recruitment, which plays a critical role in the resolution of inflammation. Intravenous BML-111 injections increase the microglia/macrophage cell populations and promote the resolution of neuroinflammation [12]. In the present study, HV_T significantly increased the numbers of macrophages/monocytes. Interestingly, an increased peak macrophage/monocyte count appeared following BML-111 administration. A main role of lung macrophages in the resolution of pulmonary inflammation is to modulate anti-inflammatory cytokine secretion, including IL-10 secretion [18]. The levels of the anti-inflammatory cytokine IL-10 were significantly increased in BML-111-treated rats subjected to HV_T.

The resolution of neutrophil-mediated inflammation occurs through apoptosis [31,32]. BML-111 promoted neutrophil apoptosis in the BALF, as evidenced by the increased annexin-V labeling in BML-111-treated rats with ventilator injury. Intriguingly, we did not observe a reduction in neutrophil apoptosis after HV_T, likely because the cytokines secreted following HV_T exerted an anti-apoptosis effect. The caspase cascade plays an important role in this process of apoptosis [17,21]. In the present study, z-VAD-fmk, a broad-spectrum caspase inhibitor, partially reversed the proapoptotic effects of BML-111 on neutrophils apoptosis and the pro-resolving effects of BML-111 on the VILI model. Although z-VAD-fmk was shown to influence cytokine secretion from macrophages [33], in our present study, z-VAD-fmk alone did not influence cytokine production, and neutrophil apoptosis or lung injury, likely because the model was different. Thus, the resolution of inflammation likely depends on neutrophil apoptosis.

Pulmonary neutrophil apoptosis is exquisitely sensitive to inflammatory mediators from the inflammatory microenvironment [34] that are regulated by various intracellular signaling pathways in the

host, including the Nrf2/HO-1 and NF-κB signaling pathways. HO-1 has been implicated in modulating the inflammatory mediators and neutrophil apoptosis in lung injury, and it participates in the resolution of acute respiratory distress syndrome [35,36]. In our study, levels of the HO-1 activity, HO-1 and Nrf2 protein expression were increased following BML-111 administration in HV_T-treated rats. The inhibitory effect of Nrf2/HO-1 on inflammation is achieved by modulating the activation of the NF-κB signaling pathway, and increased HO-1 expression inhibits NF-κB activation induced by endotoxin [5]. In the present study, the NF-κB activation and translocation induced by the one-hour HV_T treatment were inhibited by BML-111 administration, whereas ZnPPIX, a selective inhibitor of HO-1, partially reversed the inhibitory effects of BML-111 on the NF-κB signaling pathway and inflammatory mediators, in turn alleviating the proapoptotic actions of BML-111 on neutrophils apoptosis and the pro-resolving effects of BML-111 on VILI. Indeed, NF-κB inhibition accelerates the apoptosis of bovine neutrophils, whereas numerous inflammatory mediators from both microbes and the host origin inhibit this process [34,37]. Interestingly, ZnPPIX did not inhibit Nrf2 expression following the BML-111 treatment; in contrast, it upregulated Nrf2 expression. We speculate that the involvement of HO-1 in BML-111-induced suppression of NF-κB signaling is the downstream of Nrf2, but strategies inhibiting the function of HO-1 will likely stimulate a negative feedback loop that subsequently activates the Nrf2/HO-1 pathway. Therefore, the potential mechanism underlying the effects BML-111 on VILI must be further elucidated.

In conclusion, our study provides a quantitative analysis of inflammation resolution in VILI with resolution indices and reveals the moderate protection of a BML-111 posttreatment in experimental HV_T-induced VILI in terms of inflammation resolution. Based on our findings, we concluded that BML-111 promotes the resolution of inflammation caused by HV_T partially by modulating the Nrf2/HO-1 and NF-κB pathways in the lung tissue and subsequently enhancing caspase-mediated neutrophil apoptosis. Data from this study, together with data from our previous studies, indicate that the protective effect of BML-111 on VILI may be due to both the anti-inflammatory and pro-resolution properties of BML-111.

Acknowledgments

This study was supported by the National Natural Science Foundation of China (No. 81671890, 81601669).

Competing interests

The authors have declared that no competing interests exist.

References

[1] M. Vaneker, F.J. Halbertsma, J. van Egmond, M.G. Netea, H.B. Dijkman, D.G. Snijdelaar, L.A. Joosten, J.G. van der Hoeven, G.J. Scheffer, Mechanical ventilation in healthy mice induces reversible pulmonary and systemic cytokine elevation with preserved alveolar integrity: an in vivo model using clinical relevant ventilation settings, Anesthesiology 107 (3) (2007) 419–426.
[2] K.A. Brown, S.D. Brain, J.D. Pearson, J.D. Edgeworth, S.M. Lewis, D.F. Treacher, Neutrophils in development of multiple organ failure in sepsis, Lancet (London, England) 368 (9530) (2006) 157–169.
[3] S. Faller, M. Foeckler, K.M. Strosing, S. Spassov, S.W. Ryter, H. Buerkle, T. Loop, R. Schmidt, A. Hoetzel, Kinetic effects of carbon monoxide inhalation on tissue protection in ventilator-induced lung injury, Lab. Investig. 92 (7) (2012) 999–1012.
[4] D.A. Willoughby, A.R. Moore, P.R. Colville-Nash, D. Gilroy, Resolution of inflammation, Int. J. Immunopharmacol. 22 (12) (2000) 1131–1135.
[5] P.S. Tsai, C.C. Chen, P.S. Tsai, L.C. Yang, W.Y. Huang, C.J. Huang, Heme oxygenase 1, nuclear factor E2-related factor 2, and nuclear factor kappaB are involved in hemin inhibition of type 2 cationic amino acid transporter expression and L-arginine transport in stimulated macrophages, Anesthesiology 105 (6) (2006) 1201–1210 (discussion 5A).
[6] H. Pan, H. Wang, X. Wang, L. Zhu, L. Mao, The absence of Nrf2 enhances NF-kappaB-dependent inflammation following scratch injury in mouse primary cultured astrocytes, Mediat. Inflamm. 2012 (2012) 217580.
[7] D. El Kebir, J.G. Filep, Modulation of neutrophil apoptosis and the resolution of inflammation through beta2 integrins, Front. Immunol. 4 (2013) 60.
[8] C.N. Serhan, Pro-resolving lipid mediators are leads for resolution physiology, Nature 510 (7503) (2014) 92–101.
[9] C.N. Serhan, N. Chiang, T.E. Van Dyke, Resolving inflammation: dual anti-inflammatory and pro-resolution lipid mediators, Nat. Rev. Immunol. 8 (5) (2008) 349–361.
[10] N. Chiang, I.M. Fierro, K. Gronert, C.N. Serhan, Activation of lipoxin A(4) receptors by aspirin-triggered lipoxins and select peptides evokes ligand-specific responses in inflammation, J. Exp. Med. 191 (7) (2000) 1197–1208.
[11] N. Chiang, C.N. Serhan, S.E. Dahlen, J.M. Drazen, D.W. Hay, G.E. Rovati, T. Shimizu, T. Yokomizo, C. Brink, The lipoxin receptor ALX: potent ligand-specific and stereoselective actions in vivo, Pharmacol. Rev. 58 (3) (2006) 463–487.
[12] K.E. Hawkins, K.M. DeMars, J.C. Alexander, L.G. de Leon, S.C. Pacheco, C. Graves, C. Yang, A.O. McCrea, J.C. Frankowski, T.J. Garrett, M. Febo, E. Candelario-Jalil, Targeting resolution of neuroinflammation after ischemic stroke with a lipoxin A4 analog: protective mechanisms and long-term effects on neurological recovery, Brain Behav. 7(5) (2017) e00688.
[13] H. Li, Z. Wu, D. Feng, J. Gong, C. Yao, Y. Wang, S. Yuan, S. Yao, Y. Shang, BML-111, a lipoxin receptor agonist, attenuates ventilator-induced lung injury in rats, Shock 41 (4) (2014) 311–316.
[14] F.P. Conte, O. Menezes-de-Lima, Jr., W.A. Verri, Jr., F.Q. Cunha, C. Penido, M.G. Henriques, Lipoxin A(4) attenuates zymosan-induced arthritis by modulating endothelin-1 and its effects, Br. J. Pharmacol. 161(4) (2010) 911–24.
[15] Y.Z. Wang, Y.C. Zhang, J.S. Cheng, Q. Ni, P.J. Li, S.W. Wang, W. Han, Y.L. Zhang, BML-111, a lipoxin receptor agonist, ameliorates 'two-hit'-induced acute pancreatitis-associated lung injury in mice by the upregulation of heme oxygenase-1, Artif. Cells Nanomed. Biotechnol. 42 (2) (2014) 110–120.
[16] Y.Z. Wang, Y.C. Zhang, J.S. Cheng, Q. Ni, P.W. Li, W. Han, Y.L. Zhang, Protective effects of BML-111 on cerulein-induced acute pancreatitis-associated lung injury via activation of Nrf2/ARE signaling pathway, Inflammation 37 (4) (2014) 1120–1133.
[17] J. Gong, H. Liu, J. Wu, H. Qi, Z.Y. Wu, H.Q. Shu, H.B. Li, L. Chen, Y.X. Wang, B. Li, M. Tang, Y.D. Ji, S.Y. Yuan, S.L. Yao, Y. Shang, MARESIN 1 prevents lipopolysaccharide-induced neutrophil survival and accelerates resolution of acute lung injury, Shock 44(4) (2015) 371–80.
[18] N.R. Aggarwal, L.S. King, F.R. D'Alessio, Diverse macrophage populations mediate acute lung inflammation and resolution, Am. J. Phys. Lung Cell. Mol. Phys. 306 (8) (2014) L709–L725.
[19] S. Herold, K. Mayer, J. Lohmeyer, Acute lung injury: how macrophages orchestrate resolution of inflammation and tissue repair, Front. Immunol. 2 (2011) 65.
[20] G.F. Curley, M. Contreras, B. Higgins, C. O'Kane, D.F. McAuley, D. O'Toole, J.G. Laffey, Evolution of the inflammatory and fibroproliferative responses during resolution and repair after ventilator-induced lung injury in the rat, Anesthesiology 115(5) (2011) 1022–32.
[21] D. El Kebir, L. Jozsef, W. Pan, L. Wang, N.A. Petasis, C.N. Serhan, J.G. Filep, 15-Epi-lipoxin A4 inhibits myeloperoxidase signaling and enhances resolution of acute lung injury, Am. J. Respir. Crit. Care Med. 180 (4) (2009) 311–319.
[22] S.Y. Wu, S.E. Tang, F.C. Ko, G.C. Wu, K.L. Huang, S.J. Chu, Valproic acid attenuates acute lung injury induced by ischemia-reperfusion in rats, Anesthesiology 122 (6) (2015) 1327–1337.
[23] G. Matute-Bello, G. Downey, B.B. Moore, S.D. Groshong, M.A. Matthay, A.S. Slutsky, W.M. Kuebler, An official American Thoracic Society workshop report: features and measurements of experimental acute lung injury in animals, Am. J. Respir. Cell Mol. Biol. 44 (5) (2011) 725–738.
[24] G.L. Bannenberg, N. Chiang, A. Ariel, M. Arita, E. Tjonahen, K.H. Gotlinger, S. Hong, C.N. Serhan, Molecular circuits of resolution: formation and actions of resolvins and protectins, J. Immunol. (Baltimore, Md. : 1950) 174 (9) (2005) 5884c–5884.
[25] A. Korner, M. Schlegel, J. Theurer, H. Frohnmeyer, M. Adolph, M. Heijink, M. Giera, P. Rosenberger, V. Mirakaj, Resolution of inflammation and sepsis survival are improved by dietary omega-3 fatty acids, Cell Death Differ. 25 (2) (2018) 421–431.
[26] Q. Gong, H. Yin, M. Fang, Y. Xiang, C.L. Yuan, G.Y. Zheng, H. Yang, P. Xiong, G. Chen, F.L. Gong, F. Zheng, Heme oxygenase-1 upregulation significantly inhibits TNF-alpha and Hmgb1 releasing and attenuates lipopolysaccharide-induced acute lung injury in mice, Int. Immunopharmacol. 8 (6) (2008) 792–798.
[27] J. Xu, H. Hu, B. Chen, R. Yue, Z. Zhou, Y. Liu, S. Zhang, L. Xu, H. Wang, Z. Yu, Lycopene protects against hypoxia/reoxygenation injury by alleviating ER stress induced apoptosis in neonatal mouse cardiomyocytes, PLoS One 10(8) (2015) e0136443.
[28] Y.N. Xu, Z. Zhang, P. Ma, S.H. Zhang, Adenovirus-delivered angiopoietin 1 accelerates the resolution of inflammation of acute endotoxic lung injury in mice, Anesth. Analg. 112 (6) (2011) 1403–1410.
[29] M. Spite, J. Claria, C.N. Serhan, Resolvins, specialized proresolving lipid mediators, and their potential roles in metabolic diseases, Cell Metab. 19 (1) (2014) 21–36.
[30] A. Gonzalez-Lopez, G.M. Albaiceta, Repair after acute lung injury: molecular mechanisms and therapeutic opportunities, Crit. Care 16(2) (2012) 209.
[31] H. Jie, Y. He, X. Huang, Q. Zhou, Y. Han, X. Li, Y. Bai, E. Sun, Necrostatin-1 enhances the resolution of inflammation by specifically inducing neutrophil apoptosis, Oncotarget 7 (15) (2016) 19367–19381.
[32] W.C. Lin, C.F. Lin, C.L. Chen, C.W. Chen, Y.S. Lin, Inhibition of neutrophil apoptosis via sphingolipid signaling in acute lung injury, J. Pharmacol. Exp. Ther. 339 (1) (2011) 45–53.
[33] W. Martinet, D.M. Schrijvers, A.G. Herman, G.R. De Meyer, z-VAD-fmk-induced non-apoptotic cell death of macrophages: possibilities and limitations for atherosclerotic plaque stabilization, Autophagy 2 (4) (2006) 312–314.
[34] R. Taneja, J. Parodo, S.H. Jia, A. Kapus, O.D. Rotstein, J.C. Marshall, Delayed neutrophil apoptosis in sepsis is associated with maintenance of mitochondrial transmembrane potential and reduced caspase-9 activity, Crit. Care Med. 32 (7)

(2004) 1460–1469.
[35] J.J. Yuan, X.T. Zhang, Y.T. Bao, X.J. Chen, Y.Z. Shu, J.L. Chen, W. Chen, B. Du, Q.F. Pang, Heme oxygenase-1 participates in the resolution of seawater drowning-induced acute respiratory distress syndrome, Respir. Physiol. Neurobiol. 247 (2018) 12–19.
[36] X. Li, M.G. Schwacha, I.H. Chaudry, M.A. Choudhry, Heme oxygenase-1 protects against neutrophil-mediated intestinal damage by down-regulation of neutrophil p47phox and p67phox activity and O_2- production in a two-hit model of alcohol intoxication and burn injury, J. Immunol. (Baltimore, Md. : 1950) 180 (10) (2008) 6933–6940.
[37] S. Notebaert, L. Duchateau, E. Meyer, NF-kappaB inhibition accelerates apoptosis of bovine neutrophils, Vet. Res. 36 (2) (2005) 229–240.